Applied Surface Science Advances 16 (2023) 100433

Contents lists available at ScienceDirect

Applied Surface Science Advances

journal homepage: www.sciencedirect.com/journal/applied-surface-science-advances

Pinning of graphene for conformal wrinkling over a soft corrugated substrate through prestretch-release process

Mukesh Pandey [a], B.K. Parida [b], M. Ranjan [b], Rajeev Ahuja [a,c], Rakesh Kumar [*,a]

[a] Department of Physics, Indian Institute of Technology Ropar, Rupnagar, 140001, Punjab, India
[b] FCIPT, Institute for Plasma Research, Gandhinagar, 382428, India
[c] Condensed Matter Theory Group, Department of Physics and Astronomy, Uppsala University, Box 516, Uppsala, 75120, Sweden

ARTICLE INFO

Keywords:
2D materials
graphene
adhesion mechanics
wrinkling
snap through transition
conformal adhesion

MSC:
0000
1111

PACS:
0000
1111

ABSTRACT

The adhesion of a 2D material to a substrate is facilitated by the van der Waals (vdW) interactions, which is significantly influenced by the roughness and wettability of the substrate. It is challenging to achieve good as well as conformal adhesion of mechanically exfoliated 2D materials to a hydrophobic soft substrate like polydimethylsiloxane (PDMS). In addition, the mechanical folding instabilities are inevitably observed in 2D elastic nanosheets over a smooth PDMS substrate under higher compressions in a prestretch-release process. However, the manipulation of the soft substrate's surface roughness may provide an essential degree of freedom for tailoring the conformation level and topography of the 2D elastic nanosheets. Herein, we propose a technique to improve the interfacial adhesion of the graphene membrane to a periodically trenched PDMS substrate by suppressing the mechanical folding instabilities in a prestretch-release process. The conformal wrinkling of the graphene membrane, as confirmed through atomic force microscopy (AFM) imaging, is found to result from its pinning into the trenches via snap-through transition. We also show the impact of the substrate's topography on the buckling behavior of the graphene membrane under the stress loading-unloading cycle by surface-engineering of the PDMS substrate using ion beam irradiation. This study offers fundamental as well as practical insights into the adhesion mechanics of the 2D elastic nanosheets over the corrugated soft substrates under the prestretch-release process. The wrinkled topography of the membrane could be harnessed for flexible, conformal, and tunable electronic devices.

1. Introduction

The thinnest two-dimensional (2D) material, graphene shows remarkable mechanical strength as it can withstand a mechanical strain up to ~20% before rapture [1,2]. The ultra-high flexibility and stretchability of the 2D materials make them mechanically reliable and promising materials for wearable electronics [3–5]. In addition, the 2D materials show remarkably strain-sensitive electronic, optical, and vibrational properties, which make them worthy for nanoscale strain engineering [6–9]. The Nitto tape-based micromechanical exfoliation method produces 2D flakes of the highest quality amongst the other known deposition or growth techniques [10]. However, the direct transfer of single-crystalline graphene flakes (hydrophobic in nature) from the Nitto tape onto a pristine PDMS substrate faces incomplete as well as random transfer, which produces low deposition yield with several delamination regions and wrinkles [11–13]. This transfer process is probabilistic, non-deterministic, and unselective and demands the wettability of the PDMS substrate, which is hydrophobic by nature in its pristine state. For better wettability, its surface-functionalization is carried out through oxygen-plasma treatment before transfer [14]. However, it has been observed that the oxygen-plasma treatment time has a substantial effect on the surface roughness of the PDMS substrate.

The surface roughness of the underlying substrate, the number of layers in the 2D nanosheet, and the interfacial adhesion play crucial roles in the conformation or delamination of the 2D nanosheet [15–18]. Through the theoretical framework of continuum mechanics, it is found that a conformally adhered 2D nanosheet over a corrugated substrate has better debonding strength than that over a smooth and flat one [19]. The nanosheet must remain static and conformed during a mechanical straining process for an efficient and larger strain transfer. The conformity of the nanosheet is found to vary with the amplitude and wavelength of the substrate's surface corrugation. In the literature, several

* Corresponding author.
E-mail address: rakesh@iitrpr.ac.in (R. Kumar).

https://doi.org/10.1016/j.apsadv.2023.100433
Received 20 May 2023; Received in revised form 22 June 2023; Accepted 22 June 2023
Available online 1 July 2023

ways have been proposed to strengthen the interfacial adhesion between the 2D flakes and the substrates, such as (i) by polymeric encapsulation of the 2D flakes [20,21], (ii) by increasing the substrate's surface wettability [14], (iii) by anchoring the flake with metallic clamps at the edges [8], etc. These methods have their individual pros and cons. Despite extensive efforts in achieving good interfacial adhesion of 2D nanosheets, a lack of attention has been paid to the substrate's surface roughness manipulation through surface-engineering methods, possibly due to the fact that the substrate's surface roughness negatively impacts the interfacial adhesion of the 2D nanosheets. The adhesion characteristics of a 2D nanosheet over a substrate are investigated by analyzing the topographical features of the delaminated regions (blisters, folds, buckle delaminations, wrinkles, etc.) [11,22–26]. The wrinkled/buckled nano-/microstructures of 2D materials over polymeric substrates are commonly observed in thermal-mismatch-induced straining [27,28] and polymer-based transfer processes [29–34]. In addition, a significant Young's modulus mismatch between a 2D material and an elastomeric substrate results in the formation of the wrinkles of the 2D material through a conventional prestretch-release process [24,35–42]. However, the interfacial contact failure or sliding results in the formation of buckling-induced delaminations, folds, or fractures [18,43]. The physical properties of the wrinkled/buckled 2D nanosheet alter in accordance with the local deformation of the lattice structure [44]. It has been observed that the probability of the onset of the buckling-induced delamination of the 2D nanosheet reduces severely by O_2-plasma treatment of the PDMS surface [45]. The plasma treatment forms a stiff skin layer at the top of the PDMS surface but may also induce unwanted surface cracks [46]. Therefore, it is highly challenging to obtain the conformal adhesion of the 2D elastic nanosheets over hydrophobic elastomeric substrates such as PDMS.

Recently, Teng Cui *et al* [18] reported that the interfacial fatigue propagation at the graphene-polymer interface causes mechanical folding instabilities in the graphene membrane under loading-unloading cycles. The ultralow bending stiffness of the 2D materials makes them susceptible to out-of-plane buckling delamination over the stretchable substrates at small compressions due to elastic modulus mismatch. However, there is a spontaneous transition from buckle delamination to fold due to interfacial slippage at higher compression above 10% [43]. The folding instability must be suppressed in order to achieve good conformal adhesion of a 2D elastic nanosheet over a flexible substrate. The conformal and stretchable nano-/microstructures of 2D materials on flexible substrates have outstanding implications in healthcare monitoring systems, artificial electronic skins, and wearable strain/pressure sensing applications [47–49]. Current studies have been especially focussing on maximizing the structural compliance of the implanted devices [47]. The conventional electronic skins based on metal matrix have lower stability, poor compatibility with human skin, and low strain-sensing capability because of their low sensitivity and poor stretchability [50]. Graphene, on the other hand, is a very robust material for conformal artificial electronic skins due to its exceptional sensitivity, stretchability, durability, and biocompatibility. In addition, the high transparency, thermal stability, flexibility, and biocompatibility of PDMS assure the mechanical reliability of the device [51]. The PDMS (Sylgard 184) exhibits stable mechanical properties with negligible elastic hysteresis under a cyclic loading-unloading process. In addition, it immediately regains the steady state independent of the deformation rate, making it a promising substrate for wearable sensors [52]. The conformal wrinkles of single or even few-layered 2D materials over polymeric substrates allow tuning of the out-of-plane interlayer coupling in the 2D layered vdW materials to result in tunable mechanical properties [39,45], and also show remarkably enhanced mechanical, electrical, and thermal properties [47,53–57]. Despite devoted theoretical footing for the wrinkling of the 2D elastic membranes, the quest for a scalable experimental approach for creating conformal wrinkles over the corrugated soft substrates without forming folds or buckle delaminations still continues [58–60].

The conventional prestretch-release process at higher prestrain values ($\gtrsim$5%) results in the formation of folds or buckle delaminations in the 2D elastic nanosheets such as graphene, MoS_2, etc. over a smooth PDMS substrate [18,43,61]. The substrate roughness, interfacial adhesion, and elastic modulus mismatch affect the surface traction of the 2D material under compression, which determines the effective shear stress at the interface that causes buckling instability to develop. In this work, we showcase the utilization of the prestretch-release process for the pinning of the graphene membrane over periodic depressions on aPDMS substrate. We found that this technique effectively suppresses the mechanical folding instabilities in the 2D elastic nanosheets. The membrane is pinned via 'snap-through transitions'. A 'snap-through transition' occurs to change the morphology of an elastic 2D nanosheet from a flat state to a near conformal state over a corrugated substrate [62]. Similarly, a morphological switch (transition) of a buckle delamination from one stable configuration to another under the application of strain is called 'snap-through buckling instability' [63–69]. The elastic membranes are susceptible to snap-through instability in the presence of external strain [70–73]. It has been observed that the stress-transfer efficiency for graphene over a smooth & flat PDMS substrate under uniaxial stretching is as low as $\sim$ 3% [7,74] because of its weak interfacial adhesion with the PDMS substrate (~ 0.007 J /m^2) [75]. However, by exploiting the membrane pinning method, the stress-transfer efficiency can be severely enhanced. Herein, we utilized the differently rippled PDMS substrates to investigate the role of substrate roughness in the adhesion mechanics of the graphene membrane under a stress loading-unloading cycle. The ripples on the PDMS substrates are formed through low-energy ion beam (IB) irradiation at different angles of incidence [76–79]. The ripple patterns on the PDMS surface undergo morphological evolution through ion beam irradiation not only under the varying angles of incidence [77] but also under the varying ion energy [76,80] as well as the PDMS annealing temperature [81]. Our work offers fundamental as well as practical insights into the membrane pinning mechanism for conformal wrinkling over a corrugated soft substrate under the prestretch-release process at the nanoscale. This technique can be exploited to obtain hierarchical graphene architectures [39]. The regulation of the graphene configuration over the engineered surfaces opens up new pathways for conformal and tunable electronics [66,79,82].

2. Results and Discussion

The conventional prestretch-release process (as depicted in Fig. 1) has been extensively utilized for controlled buckling of the 2D elastic nanosheets [35–37]. The micromechanically exfoliated single or few-layer graphene (SLG/FLG) flakes (hydrophobic in nature) are deposited onto a prestretched (by 40% of original length) PDMS substrate having a flat or rippled surface (see Fig. 2) by employing the 'PVA-assisted wet transfer process'. Due to the large elastic modulus mismatch between the graphene membrane and the PDMS substrate ($10^6 : 1$), periodic wrinkles (conformal deformation of the membrane and the substrate) or buckle delaminations develop over the substrate upon release of the prestrain.

The interfacial behavior in the context of the substrate's roughness and slipperiness has an impact on the buckling topography of a 2D elastic nanosheet, in addition to the elastic properties of the 2D material, thickness of the nanosheet, and the amount of compressive stress [18,43,83] (see Figure S3 of ESI). Now, in order to analyze the role of substrate surface corrugation in the adhesion mechanics of the graphene flakes under the prestretch-release process, we utilize the PDMS substrates rippled or patterned through IB irradiation. The low-energy (500 eV) argon ion beams, incident on the pristine PDMS substrate at different incident angles, produce surface ripples of different corrugation profiles as a result of the stress-driven instabilities. For the IB irradiation at the angles of incidence of 0° and 60° to the normal to the PDMS surface, we

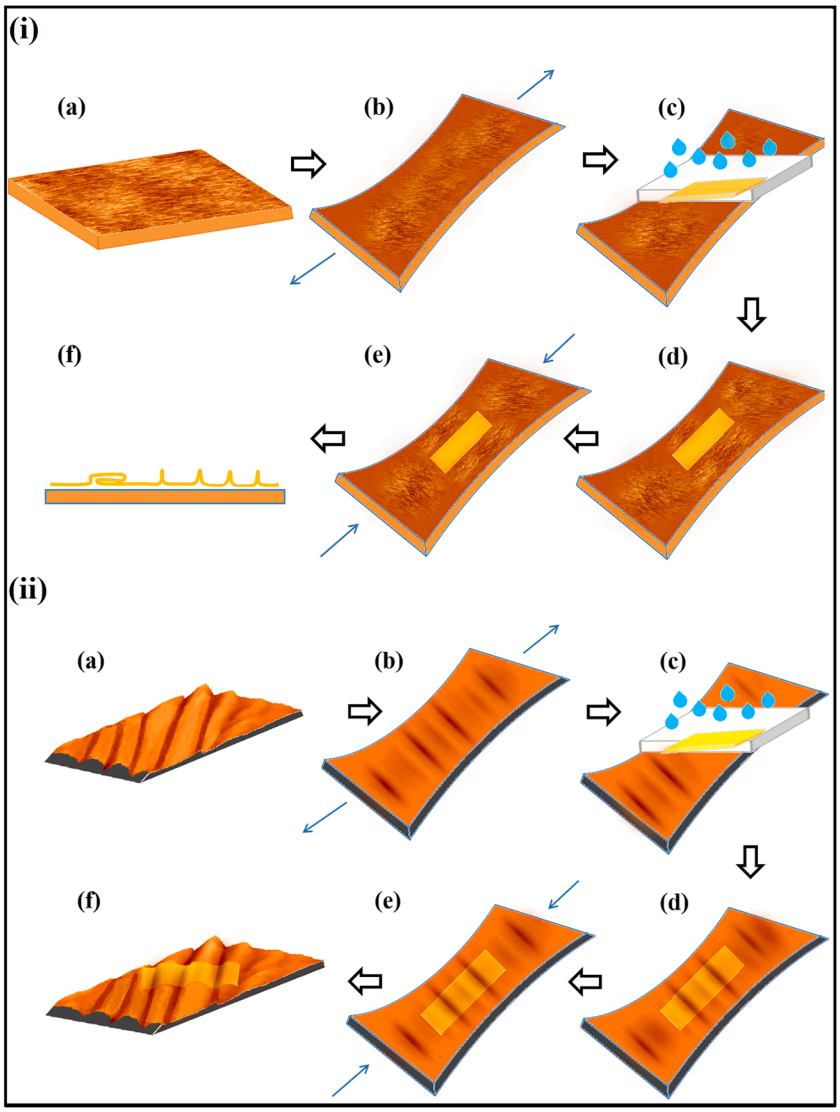

Fig. 1. Schematics showing (i) the buckling-induced folds and delaminations of a 2D elastic membrane over a flat & smooth surface of PDMS, and (ii) the conformal wrinkling of a 2D elastic membrane over a corrugated surface of PDMS, resulting from the conventional prestretch-release process.

obtained serpentine-shaped ripples (see Fig. 2(b & d, respectively)), but interestingly, at an angle of incidence of around 30° a nearly periodic trench (depression) pattern in addition to the ripples is obtained on the PDMS surface (see Fig. 2 (c)). The competition between the bending energy of the homogeneous silica-like stiff skin layer (formed due to ion beam irradiation) and the stretching energy of the soft supporting layer of PDMS plays a crucial role in determining the ripple parameters or the corrugation profile [77]. The ion beam collision-induced local heating effect increases the local degree of crosslinking in the PDMS, which varies with the angle of incidence of the ion beam. As the degree of crosslinking increases, the number of polymeric chains in the PDMS decreases. Consequently, its stiffness (toughness) increases and the free volume in the polymer decreases locally, which restricts the local movement of the reactive ions. The thermal effect-driven restriction in the movement of the ions would reduce their penetration depth into the PDMS substrate [81]. The penetrating energetic ions collide with the PDMS structure and thereby, erode the molecules out of the structure. After the reorganization of the atoms on the surface, thinner silica-like skin layers form in the PDMS substrate, which results in the formation of ripples of smaller corrugation wavelengths. Therefore, a competitive interplay between the sputtering-induced self-diffusion and thermally activated self-diffusion processes determines the growth dynamics of the surface instability in the form of ripples [84].

We observed folds of SLG/FLG flakes not only over the smooth PDMS substrate but also over the randomly oriented serpentine ripples on the PDMS substrates (obtained from argon ion beam incident angles: 0° and 60°) in the uniaxial prestrain-release process with a prestrain level of40% (see Fig. 3). The compressive stress resulting from the uniaxial loading-unloading cycle leads to local activation of the buckle delamination regions alongside the existing wrinkles, which spontaneously collapse to form the folds [18]. The collapsed folds appear as white belts through high-resolution optical microscopy [43] (see Figures S2 and S3 of ESI). The wrinkle-to-fold transition occurs due to interfacial sliding in a stress-release process for a significant prestrain level [18]. The prestretch-release process not only induces the buckling zone but also propagates the buckle wave-fronts dynamically from the edges toward the internal region, and the wrinkle-to-fold transition occurs in the buckling zone. The ultra-low bending stiffness and high self-adhesion of the single to few-layer graphene flakes give rise to the formation of the hair-pin-shaped folds, however, the buckle delaminations are more pronounced for the multilayered flakes [43]. We noticed that as the roughness of the PDMS surface increases the density of the graphene folds decreases with the increasing width of the folds due to rising friction under compression (see Fig. 3). The roughness of the substrate

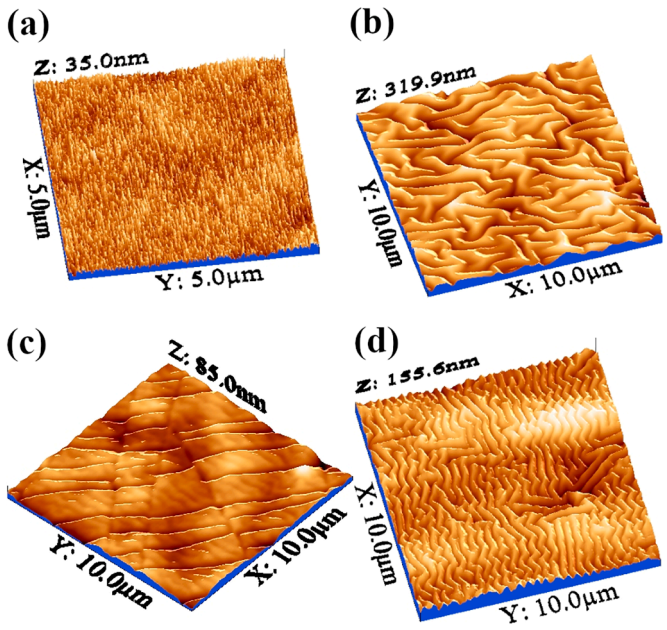

Fig. 2. AFM topographic 3D images of (a) the flat & smooth surface of a pristine PDMS substrate, and (b, c, and d) rippled PDMS surfaces obtained through IB irradiation at angles of incidence of 0°, 30°, and 60°, respectively, with respect to a normal to the PDMS substrate's surface.

influences the interplay of interfacial slippage and delamination under compression. As the compressive stress reaches a threshold value (σ_{thr}) at a point, the delamination of the membrane occurs spontaneously, depending upon the interfacial adhesion energy (Γ) of the 2D elastic membrane and the substrate, such that [43]

$$\sigma_{thr} = \sqrt{2E_{2D}\Gamma}. \quad (1)$$

Hence, it is possible to suppress the mechanical folding instabilities in 2D elastic nanosheets under compression by altering the interfacial adhesion by means of manipulating the substrate's surface roughness. It is therefore compelling to search for an appropriate surface feature that can offer a conformal as well as durable adherence to the graphene membrane without causing any folding instability. Interestingly, we observed conformal wrinkles of graphene flakes (which are free from folds) over periodically trenched PDMS surfaces obtained with IB irradiation at an incident angle of around30° (see Figs. 4 and 5). We note that almost equally & parallelly spaced unidirectional depressions (trenches), having a maximum wavelength of ∼ 0.5 μm and a maximum depth of ∼ 50 nm, on the ion-irradiated surface of the PDMS, help in the conformal wrinkling of SLG/FLG flakes under the prestretch-release process. The degree of conformation of a membrane having single to few atomic layers of carbon atoms (SLG/FLG flake) increases with an increase in the corrugation wavelength of a periodically rippled substrate [19]. It has been observed that single-layer graphene conforms more closely to a corrugated substrate having a larger curvature [85,86]. Therefore, a larger corrugation wavelength of the depressions on the PDMS substrate would prevent the atomically thin 2D flakes from forming folds under the prestretch-release process. This indicates that a better conformation of the graphene flakes is expected over a 'corrugated PDMS substrate in a prestretched state' in comparison to its normal state. When uniaxial tensile stress is applied in a direction normal to the axis of the periodic depressions in the plane of the trenched PDMS surface prior to the deposition of graphene, the depressions become shallower & broader (see Fig. 4(i)-b). The shallower depressions allow the graphene membrane to conform more closely, which thereby helps in its conformal wrinkling under compression while the prestrain is released (see Fig. 4). The graphene membrane does not conform close enough to the trenches over the PDMS surface directly, but under extension, the trenches broaden enough to make the membrane snap-through due to interfacial slippage. When the prestretched PDMS substrate is released, the pinning of the membrane over the periodic trenches takes place. As a result, the membrane adheres to the trenches conformally. As a consequence, the graphene membrane conformally adheres to the protrusions in the neighborhood of the trenches on the PDMS substrate without forming folds or buckle delaminations.

It should be noted that the thickness of the soft PDMS substrate is sufficiently large in comparison to that of the graphene membrane, which is consistent with the thin-film buckling theory [18,87]. The

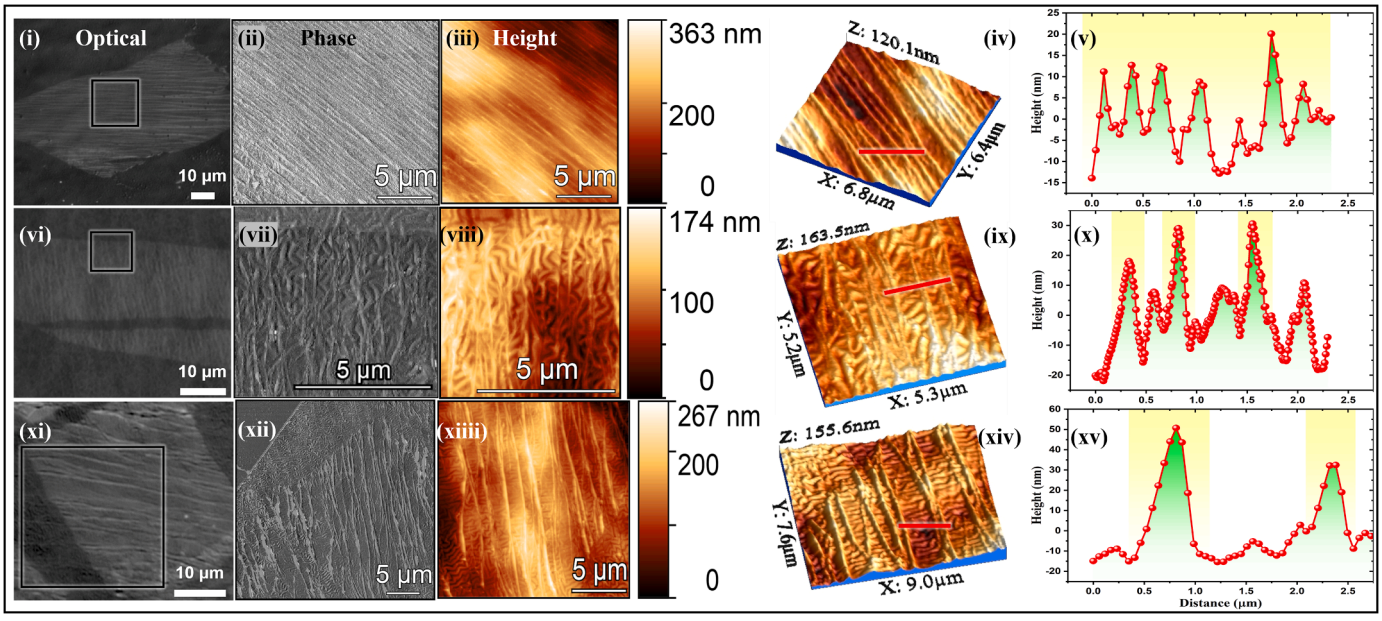

Fig. 3. Optical, AFM phase, 2D & 3D height images, and corresponding line profiles across the lines marked in red (respectively, from left to right in a row) of the graphene flakes (single to few layers) over the smooth (i-v), and rippled PDMS surfaces obtained through IB irradiation at the angles of incidence of 0° (vi-x), and 60° (xi-xv). The optically visible white belts across the graphene flakes depict the buckling-induced folds. The shaded portions in graphs represent the graphene folds distinguishing it from the PDMS surface corrugations.

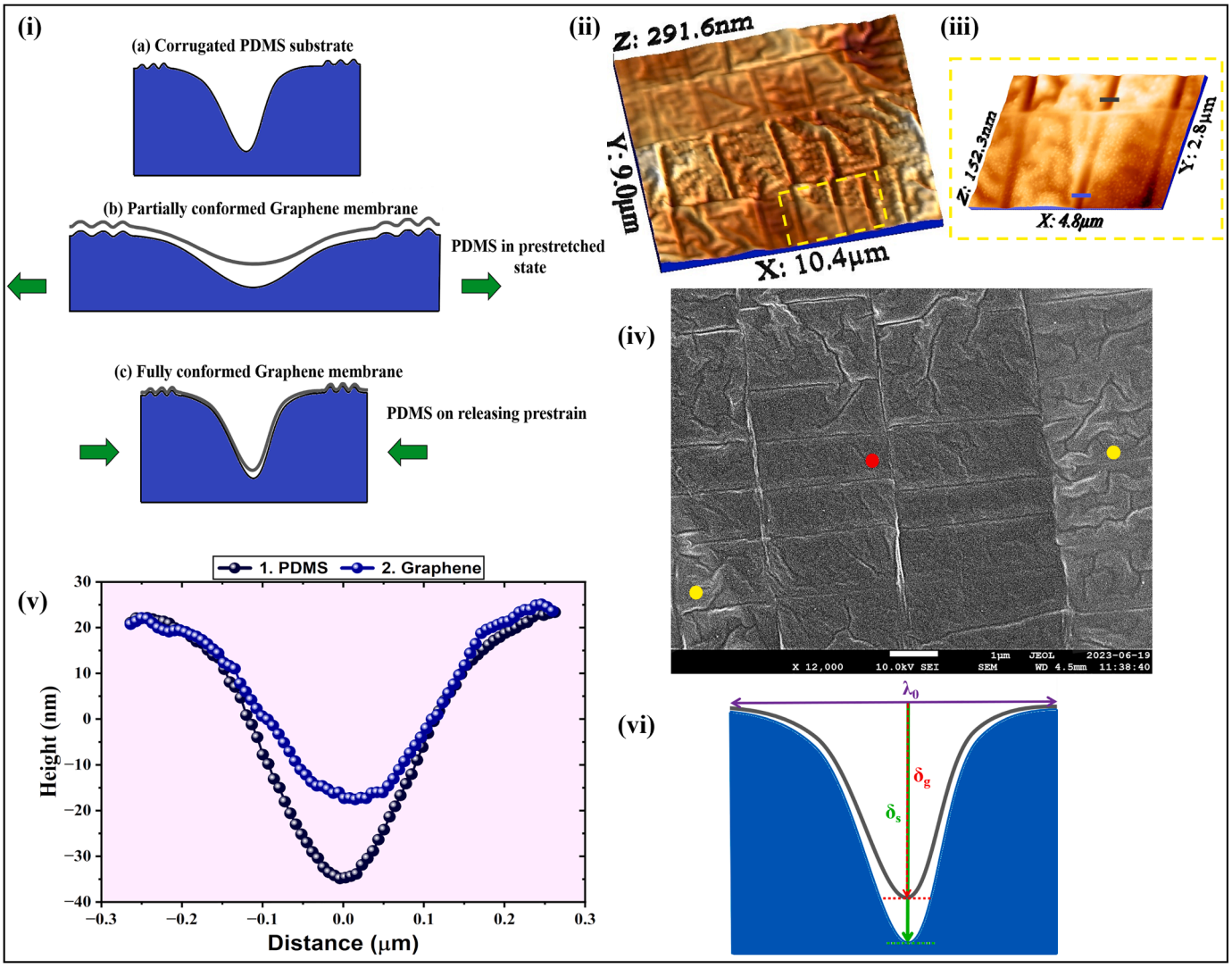

Fig. 4. (i) Pinning of graphene membrane over the corrugated PDMS substrate via snap-through transition under the prestretch-release process. (ii) AFM topographic 3D image of the wrinkled graphene over a corrugated PDMS substrate having trenches, obtained through IB irradiation at an angle of incidence of 30°. (iii) Zoomed-in AFM topographic 3D image of the wrinkled graphene over trenches. (iv) FESEM image of the wrinkled graphene on the corrugated PDMS substrate (the red point indicates the wrinkled graphene region, and the yellow point indicates the corrugated PDMS region). (v) Topographic pinned configuration of the graphene membrane over a periodic depression. The line profiles correspond to the lines marked in black (for PDMS trench) and blue (for graphene wrinkle) in figure (iii). (vi) A schematic representation of the pinned configuration.

critical compressive stress for the onset of the wrinkling is given by, $\sigma_c = \frac{\widetilde{E}_g}{4}\left(\frac{3\widetilde{E}_s}{\widetilde{E}_g}\right)^{2/3}$, where E_s and E_g are Young's modulus of the PDMS substrate and the graphene membrane, respectively, and $\widetilde{E} = \frac{E}{1-\nu^2}$, where ν is the Poisson's ratio [83]. The wrinkling is favored for $\sigma > \sigma_c$. The release of the prestrain leads to the development of purely sinusoidal wrinkles of the graphene flake of thickness τ with a wrinkle amplitude $\delta_0 = \tau\sqrt{\frac{\sigma}{\sigma_c} - 1}$, and a wrinkle wavelength $\lambda_0 = 2\pi\tau\left(\frac{\widetilde{E}_g}{3\widetilde{E}_s}\right)^{1/3} = \frac{\pi\tau}{\sqrt{\varepsilon}}$, where $\varepsilon = \sigma_c/\widetilde{E}_g$, is the elastic modulus mismatch strain. Under the prestretch-release process with a significant prestrain level of 40%, the wrinkle-to-buckle delamination transition would have begun at the lower values of compression, but at the later stages of the compression, the buckle comes into closure proximity due to vdW interactions and snaps into the form of a fold on the slippery interface [18,70].

The out-of-plane bending energy, in-plane strain (stretch/compression) energy, pinning (adhesion) energy of the graphene membrane, and surface roughness of the corrugated substrate play crucial roles in determining the equilibrium configuration profile (pinned or depinned) of the membrane over the corrugated soft substrate. As the Föpple von Kármán (FvK) number (bendability) of the layered 2D materials is very large, i.e. $\kappa = \frac{E_{2D}a^2}{B_{\text{eff}}} \gg 1$, where $B_{\text{eff}} = \frac{E\tau^3}{12(1-\nu^2)} \approx \frac{NEt^3}{12(1-\nu^2)}$ is the effective out-of-plane bending stiffness (as each layer of a layered 2D material bends independently [88,89]), and $E_{2D} = E\tau$ is the in-plane (2D) elastic strain stiffness of the graphene membrane of thickness $\tau = Nt$, having the number of layers N, Young's modulus E, the Poisson's ratio ν, and the thickness of each layer of graphene t. In this case, the in-plane elastic strain energy dominates over the out-of-plane bending energy. The length scale parameter in the continuum model [90], i.e. $l = \sqrt{\frac{B_{\text{eff}}}{E_{2D}}}$, determines a crossover from the bending rigidity-dominated regime ($\delta_g < l$) to the in-plane strain-dominated regime ($\delta_g > l$), where δ_g is the corrugation amplitude of the graphene membrane. For the standard elastic parameters of single-layer graphene, $l \approx 0.1$ nm, which implies that the elastic in-plane strain-dominated regime is more favorable for graphene. This regime favors the pinned configuration of graphene over the trenched PDMS substrate, which is attained via its snap-through transition over the shallower depressions [90].

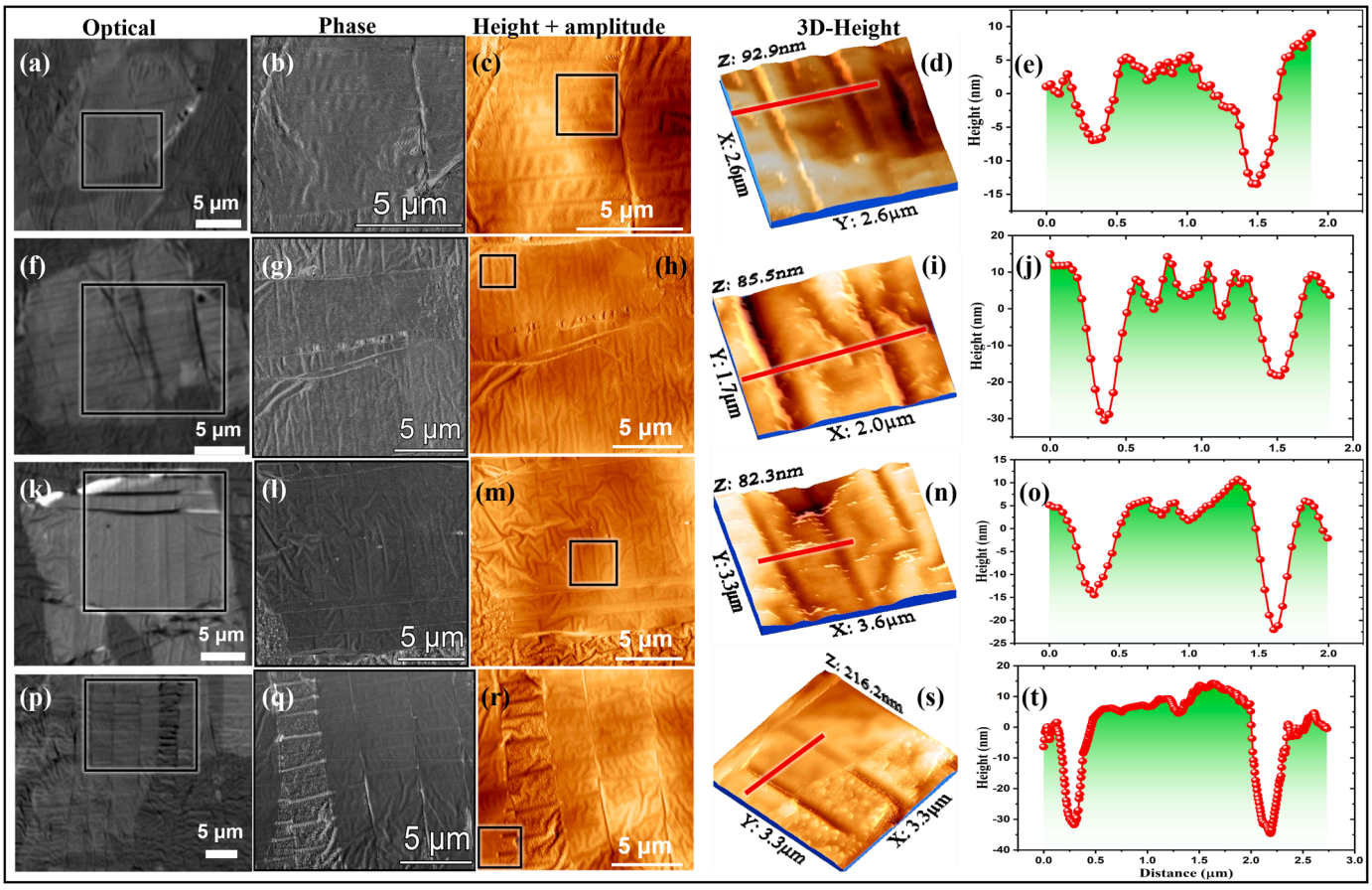

Fig. 5. Optical, AFM phase, superimposed height & amplitude, zoomed-in 3D height images, and corresponding line profiles, across the lines marked in red, (respectively, from left to right in a row) of the wrinkled graphene (SLG (a, p) & FLG (f, k)) flakes over the trenched PDMS substrates obtained through IB irradiation at an angle of incidence of 30°. Note that the mechanical folding instabilities are suppressed effectively.

At the snap-through condition, the pinning or interfacial adhesion energy of the graphene membrane becomes equal to its elastic strain energy over the trenched PDMS substrate, and the morphological transition occurs from the less conformal (or flat) state to the more conformal state, as depicted in Fig. 4(i)-b. The elastic modulus mismatch-induced out-of-plane buckling or folding under in-plane compression is suppressed due to pinning of the graphene membrane over the trenches (depressions) on the rippled PDMS substrate via snap-through instability [64] (see Fig. 5). For the corrugated graphene membrane having corrugation amplitude δ_g and corrugation wavelength over a trenched PDMS substrate, the out-of-plane bending energy is given by $E_b \sim B_{\text{eff}} \frac{\delta_g^2}{\lambda_0^2}$, and the in-plane elastic stretching energy is $E_s \sim E_{2D} \frac{\delta_g^4}{\lambda_0^2}$ [19,90]. The interfacial adhesion (pinning) energy density of the graphene membrane is $\Gamma_0 \sim E_{\text{pin}}/\lambda_0^2$. The competitive interplay between the aspect ratio $\left(\frac{\delta_g}{\lambda_0}\right)$ and the elasticity of the corrugated membrane determines the configuration (pinned or depinned) of the membrane over the corrugated substrate. In the regime ($\delta_g > l$), where the elastic in-plane strains are dominant and also responsible for the depinning of the membrane [90], the membrane favors the pinned configuration in the limit $\frac{E_{\text{pin}}}{E_s} > 1$, which results in (simplified approximation)

$$\frac{\delta_g}{\lambda_0} < \left(\frac{\Gamma_0}{E_{2D}}\right)^{\frac{1}{4}}. \tag{2}$$

This infers that the shallower depression favors the pinning of the membrane under the prestretch-release process (see Fig. 4(i)-b) [90]. The pinned configuration is always a local minimum of the total energy of the system. As a simplified assumption, a conformally adhered graphene membrane on a sinusoidally corrugated PDMS surface, having a corrugation wavelength of λ_0 and corrugation amplitude δ_s, attains a corrugation amplitude of δ_g due to vdW interactions (as shown in Fig. 4 (vi)). For fully conformal wrinkles, the corrugation amplitude of graphene equals to that of the substrate, i.e. $\delta_g \approx \delta_s$. From the minimization of the total free energy of the system (by following the approach by Aitken and Huang [19]), the interfacial adhesion energy density (Γ_0) of the membrane, having an equilibrium separation h_0 from the substrate's surface in the pinned state, turns out to be [19,60,62] (see Section I: ESI)

$$\frac{\Gamma_0}{E_{2D}} \sim \frac{1}{24}\left(\frac{2\pi\delta_g}{\lambda_0}\right)^4. \tag{3}$$

For the pinned graphene membrane over the trenched PDMS substrate in our experiment, the above equation 3 yields the interfacial adhesion energy of the order of 2.2 J/m^2. The adhesion strength is almost 5 times larger than that reported for monolayer graphene on a smooth silicon oxide substrate [91]. The ultrastrong adhesion of the graphene membrane over the soft corrugated substrate results from the pinning effect. An increase in the corrugation wavelength while prestretching the trenched PDMS substrate favors the snap-through transition of the membrane from flat morphology to a conformal state, which gives rise to the pinning effect while releasing the prestrain. Though the degree of interfacial adhesion improves via the optimized substrate's surface engineering through the prestretch-release process, but in order to release any residual strain and to attain a fully conformal state of the graphene wrinkles over the rippled PDMS surface with periodic depressions, repeated stress loading-unloading cycles could be performed [7,92]. We analyzed the strain distribution across the

wrinkled single-layer graphene under the varying applied tensile strain in the clamped PDMS substrate using a two-point bending/stretching tool (as shown in Fig. 6) with in-situ μ-Raman mapping. The characteristic 2D peak is typically found to red-shift up to a tensile strain level of 40% applied uniaxially across the adhered graphene flake. Since the laser spot size ($\sim 1\ \mu$m) is not consistent with the corrugation wavelength or width ($\lesssim 0.5\ \mu$m) of the wrinkles, the acquired Raman signals mainly manifest the strain distribution across the flat regions of the wrinkled flake. As an estimate, the flat regions of wrinkled graphene experience a uniaxial tensile strain of $\sim 0.2\%$ [36,93] at an applied tensile strain level of 40% (see Fig. 6(f)). On stretching the trenched PDMS substrate uniaxially, the corrugation amplitude (depth) of the depressions on the substrate's surface would reduce to match the corrugation amplitude of the graphene membrane, which would further strengthen the interfacial bonding. The stronger conformation of graphene would reduce the probability of the graphene wrinkles to alter their orientation during loading-unloading cycles [94]. Such a wrinkled architecture obtained via the pinning of graphene over the trenched PDMS substrate could be beneficial for conformal and tunable electronics.

3. Conclusion

In summary, the corrugation profile of the polymeric substrate plays a crucial role in the buckling of the 2D elastic nanosheet under the prestretch-release process. The mechanical folding instabilities in the graphene membrane over a flat & smooth flexible substrate are inevitably observed at higher compressions in the prestretch-release process due to a significant elastic modulus mismatch. On the contrary, the snap-through transition of the graphene membrane across the shallower & nearly periodic depressions (trenches) on a prestretched PDMS substrate helps in the conformal wrinkling of the membrane on releasing the prestrain. Hence, we present a technique to manipulate the corrugation profile of a trenched soft substrate using the prestretch-release procedure to suppress the mechanical folding instabilities and thereby achieve conformal adherence of the graphene membrane through the pinning mechanism. This work opens up new pathways for achieving the substrate-regulated morphologies of the 2D elastic nanosheets. The conformal wrinkling of the 2D nanosheets may be harnessed for designing functional nanoelectromechanical conformal devices.

4. Experimental methods

4.1. Fabrication of PDMS substrates

First, the silicone elastomer base and silicone elastomer curing agent of the Dow Corning SYLGARD-184 kit (Sigma Aldrich) taken in a 10:1 ratio by mass, are properly mixed in a petri-dish for 10 min to make a homogeneous solution. The solution is kept inside a vacuum desiccator for 5 min to pop out the bubbles formed in the PDMS solution during the

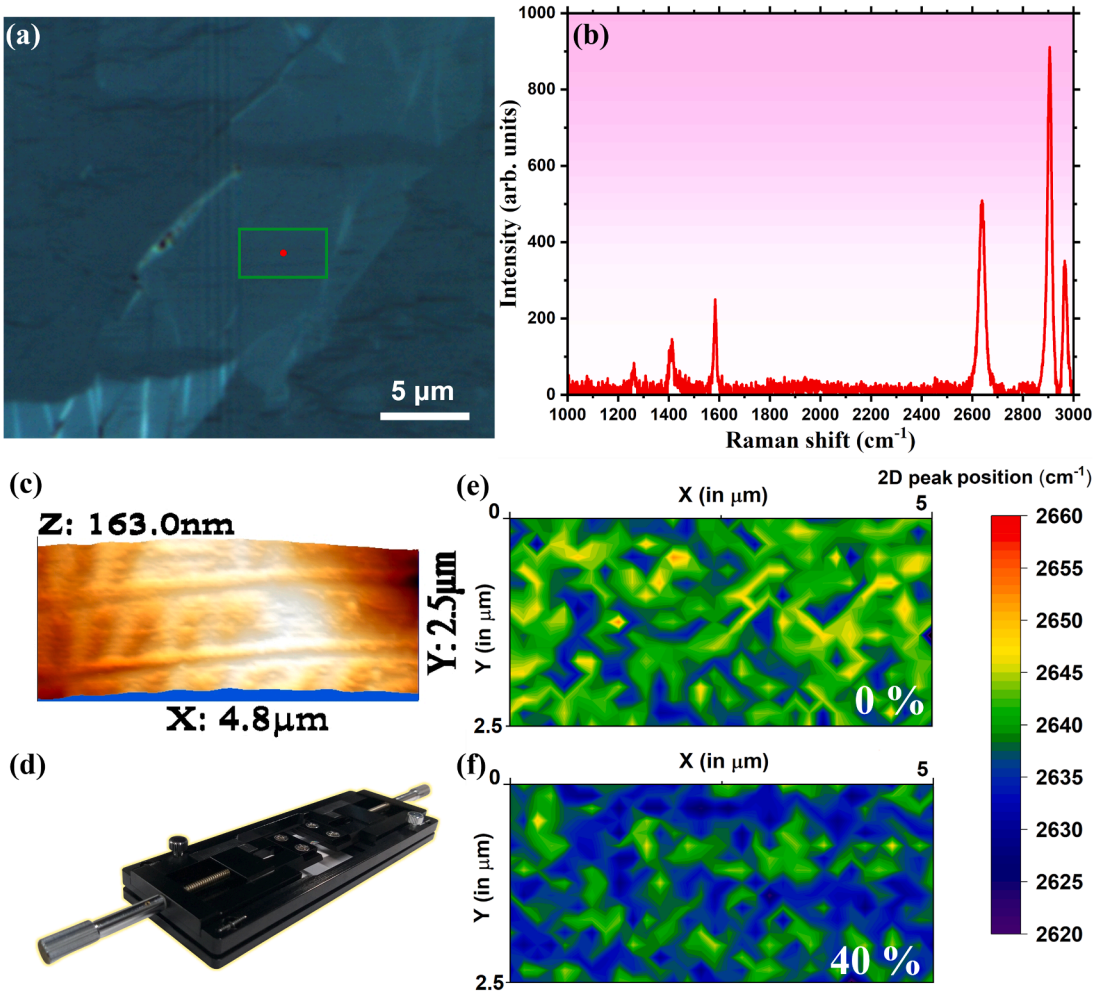

Fig. 6. (a) Optical image of wrinkled single-layer graphene over a trenched PDMS substrate, (b) the corresponding Raman spectrum taken at a point, (c) AFM 3D height image of the wrinkled graphene flake, (d) a two-point uniaxial straining tool, and (e, f) Raman maps of 2D peak position for the area indicated by the green square in figure (a) under the applied tensile strain-level of (e) 0%, and (f) 40%, respectively.

stirring. The mixture is then spin-coated at 200 rpm for 90 s on a 4-inch borosilicate glass wafer to ensure better flattening of the polymer surface. The spin-coated PDMS is cured in a convection oven at 100°C for 1 h after letting it settle down for 10 min. The PDMS film is peeled from the wafer once it cools down to room temperature. The PDMS sheet ($\sim 250\ \mu$m thick) is cut into smaller sheets of dimensions 1 cm × 1 cm to use as flexible substrates for further investigation.

4.2. Ion-beam bombardment assisted rippling of PDMS substrates

Low energy (500 eV) argon ion beams, extracted from a Kaufman-type broad-beam ion source, are incident on a pristine flat/smooth PDMS substrate. All experiments are conducted in an ultra-high vacuum (UHV) chamber of base pressure 8×10^{-8} mbar and working pressure of 1×10^{-4} mbar. To avoid the impurity, special care has been taken using the load lock system attached to the UHV chamber. The ion flux is set to 2.87×10^{15} ions/cm^2/s, the ion fluence is set to 8.62×10^{17} ions /cm^2, and the angle of incidence of the ion beam with respect to a normal to the PDMS substrate's surface is set to 0°, 30°, and 60°, sequentially, each for a bombardment period of 5 min. We obtain the surface nanoripples of different corrugation profiles. The pristine PDMS substrate surface has a root mean square (RMS) roughness of ∼ 5 nm. Ion beam (IB) irradiation, however, causes the RMS roughness to dramatically increase up to ∼ 30 nm.

4.3. Sample fabrication and PVA-assisted wet transfer process

PVA-assisted exfoliation (PAE) technique is used to deposit graphene flakes onto a PVA-coated borosilicate glass (Pyrex) substrate [25,95], wherein the deposition of the high-quality single-crystalline graphene flakes from a Nitto tape decorated with graphitic flakes in conformal contact with the substrate takes place while curing the PVA film. The graphene/PVA/Pyrex stack, in upside-down orientation, is aligned & placed in conformal contact with a smooth or rippled prestretched-(poly)dimethylsiloxane (p-PDMS) substrate (uniaxially stretched by 40% of its length using a two-point stretching tool). The PVA film is dissolved with continuously but gradually falling DI water droplets over it for ∼ 6 h at room temperature, which thereby leaves behind the graphene flakes on the p-PDMS substrate. No water intercalation between the graphene flakes and the PDMS substrate (as both are hydrophobic by nature) helps the water-soluble layer of PVA to get dissolved properly, and a clean & complete transfer of the graphene flakes is obtained with their unaltered relative positions. The graphene/p-PDMS stack, held with the straining stage, is then dried overnight under reduced pressure for better adhesion. Thereafter, the uniaxially prestretched PDMS substrate is released controllably, which generates periodic wrinkles or buckle delaminations of the graphene flakes on the PDMS substrate (see Fig. 1).

4.4. Characterizations

Optical identification of the graphene flakes has been carried out under a high-resolution optical microscope. The Raman spectroscopic measurements have been carried out using a HORIBA LabRAM HR Evolution system on the identified 2D flakes in ambient atmospheric conditions. The output power of the laser light is kept low (to avoid local heating) at ∼ 1 mW for the laser excitation wavelength of 633 nm using a 100 × air objective lens (NA=0.8) with a detector grating of 600 lines mm^{-1} in a confocal microscopy setup. The laser spot size is of the order of 1 μm. For the Raman mapping, the acquisition time is set to 1 s for single accumulation with a step size of 160 nm. The atomic force microscopy (AFM)-based topographical measurements have been performed with a standard silicon cantilever (in tapping mode) on a Bruker MultiMode-8 AFM setup. The AFM data visualizations and analyses have been carried out using the Gwyddion and WSxM software packages. The field emission scanning electron microscopy (FESEM) images of the samples (after gold coating) were captured with JEOL JSM-7610F Plus setup for morphological characterization.

CRediT authorship contribution statement

Mukesh Pandey: Conceptualization, Data curation, Formal analysis, Investigation, Methodology, Validation, Visualization, Writing – original draft, Writing – review & editing. **B.K. Parida:** Investigation, Validation. **M. Ranjan:** Writing – review & editing. **Rajeev Ahuja:** Writing – review & editing. **Rakesh Kumar:** Supervision, Writing – review & editing.

Declaration of Competing Interest

The authors declare that they have no known competing financial interests or personal relationships that could have appeared to influence the work reported in this paper.

Data availability

Data will be made available on request.

Acknowledgements

The authors (M.P., R.K.) would like to acknowledge the Central Research Facility (CRF), IIT Ropar for AFM, FESEM, Raman & PL measurements. One of the authors (M.P.) would like to thank the Ministry of Education (MoE), Govt. of India, for financial support. R.A. acknowledges the Swedish Research Council (VR-2016-06014 & VR-2020-04410), J. Gust. Richert stiftelse, Sweden (2021-00665), and SNIC (2021/1-42 and 2022/1-34) Sweden for support.

Supplementary material

Supplementary material associated with this article can be found, in the online version, at 10.1016/j.apsadv.2023.100433

References

[1] A.K. Geim, K.S. Novoselov, The rise of graphene, Nature Materials 6 (3) (2007) 183–191, https://doi.org/10.1038/nmat1849.
[2] M. Pandey, C. Pandey, R. Ahuja, R. Kumar, Straining techniques for strain engineering of 2d materials towards flexible straintronic applications, Nano Energy 109 (2023) 108278, https://doi.org/10.1016/j.nanoen.2023.108278.https://www.sciencedirect.com/science/article/pii/S2211285523001143
[3] L. Gao, Flexible device applications of 2d semiconductors, Small 13 (35) (2017) 1603994.https://doi.org/10.1002/smll.201603994
[4] J.-H. Ahn, B.H. Hong, Graphene for displays that bend, Nature Nanotechnology 9 (10) (2014) 737–738, https://doi.org/10.1038/nnano.2014.226.
[5] N. Patil, A. Gupta, M. Jaiswal, S. Dutta, Chemical-free transfer of patterned reduced graphene oxide thin films for large area flexible electronics and nanoelectromechanical systems, Nanotechnology 31 (49) (2020) 495301, https://doi.org/10.1088/1361-6528/abb26b.
[6] D. Akinwande, N. Petrone, J. Hone, Two-dimensional flexible nanoelectronics, Nature Communications 5 (1) (2014) 5678, https://doi.org/10.1038/ncomms6678.
[7] T. Jiang, R. Huang, Y. Zhu, Interfacial sliding and buckling of monolayer graphene on a stretchable substrate, Advanced Functional Materials 24 (3) (2014) 396–402, https://doi.org/10.1002/adfm.201301999.
[8] H.J. Conley, B. Wang, J.I. Ziegler, R.F. Haglund, S.T. Pantelides, K.I. Bolotin, Bandgap engineering of strained monolayer and bilayer mos2, Nano Letters 13 (8) (2013) 3626–3630, https://doi.org/10.1021/nl4014748.PMID: 23819588
[9] S. Deng, A.V. Sumant, V. Berry, Strain engineering in two-dimensional nanomaterials beyond graphene, Nano Today 22 (2018) 14–35, https://doi.org/10.1016/j.nantod.2018.07.001.http://www.sciencedirect.com/science/article/pii/S1748013217306345
[10] Y. Huang, Y.-H. Pan, R. Yang, L.-H. Bao, L. Meng, H.-L. Luo, Y.-Q. Cai, G.-D. Liu, W.-J. Zhao, Z. Zhou, L.-M. Wu, Z.-L. Zhu, M. Huang, L.-W. Liu, L. Liu, P. Cheng, K.-H. Wu, S.-B. Tian, C.-Z. Gu, Y.-G. Shi, Y.-F. Guo, Z.G. Cheng, J.-P. Hu, L. Zhao, G.-H. Yang, E. Sutter, P. Sutter, Y.-L. Wang, W. Ji, X.-J. Zhou, H.-J. Gao, Universal mechanical exfoliation of large-area 2d crystals, Nature Communications 11 (1) (2020) 2453, https://doi.org/10.1038/s41467-020-16266-w.

[11] C.J. Brennan, J. Nguyen, E.T. Yu, N. Lu, Interface adhesion between 2d materials and elastomers measured by buckle delaminations, Advanced Materials Interfaces 2 (16) (2015) 1500176, https://doi.org/10.1002/admi.201500176.
[12] B. Jayasena, S.N. Melkote, An investigation of pdms stamp assisted mechanical exfoliation of large area graphene, Procedia Manufacturing 1 (2015) 840–853, https://doi.org/10.1016/j.promfg.2015.09.073.43rd North American Manufacturing Research Conference, NAMRC 43, 8-12 June 2015, UNC Charlotte, North Carolina, United States
[13] Z. Chen, J. Biscaras, A. Shukla, Optimal light harvesting in 2d semiconductor heterostructures, 2D Materials 4 (2) (2017) 025115, https://doi.org/10.1088/2053-1583/aa736f.
[14] F. Du, H.L. Duan, C.Y. Xiong, J.X. Wang, Substrate wettability requirement for the direct transfer of graphene, Applied Physics Letters 107 (14) (2015) 143109, https://doi.org/10.1063/1.4932655.
[15] J. Bunch, M. Dunn, Adhesion mechanics of graphene membranes, Solid State Communications 152 (15) (2012) 1359–1364, https://doi.org/10.1016/j.ssc.2012.04.029.Exploring Graphene, Recent Research Advances
[16] M.B. Elinski, Z. Liu, J.C. Spear, J.D. Batteas, 2d or not 2d? the impact of nanoscale roughness and substrate interactions on the tribological properties of graphene and mos2, Journal of Physics D: Applied Physics 50 (10) (2017) 103003, https://doi.org/10.1088/1361-6463/aa58d6.
[17] Z. Lu, M.L. Dunn, van der waals adhesion of graphene membranes, Journal of Applied Physics 107 (4) (2010) 044301, https://doi.org/10.1063/1.3270425.
[18] T. Cui, K. Yip, A. Hassan, G. Wang, X. Liu, Y. Sun, T. Filleter, Graphene fatigue through van der waals interactions, Science Advances 6 (42) (2020) eabb1335, https://doi.org/10.1126/sciadv.abb1335.
[19] Z.H. Aitken, R. Huang, Effects of mismatch strain and substrate surface corrugation on morphology of supported monolayer graphene, Journal of Applied Physics 107 (12) (2010) 123531, https://doi.org/10.1063/1.3437642.
[20] F. Carrascoso, H. Li, R. Frisenda, A. Castellanos-Gomez, Strain engineering in single-, bi- and tri-layer mos2, mose2, ws2 and wse2, Nano Research 14 (6) (2021) 1698–1703, https://doi.org/10.1007/s12274-020-2918-2.
[21] Z. Li, Y. Lv, L. Ren, J. Li, L. Kong, Y. Zeng, Q. Tao, R. Wu, H. Ma, B. Zhao, D. Wang, W. Dang, K. Chen, L. Liao, X. Duan, X. Duan, Y. Liu, Efficient strain modulation of 2d materials via polymer encapsulation, Nature Communications 11 (1) (2020) 1151, https://doi.org/10.1038/s41467-020-15023-3.
[22] D.A. Sanchez, Z. Dai, P. Wang, A. Cantu-Chavez, C.J. Brennan, R. Huang, N. Lu, Mechanics of spontaneously formed nanoblisters trapped by transferred 2d crystals, Proceedings of the National Academy of Sciences 115 (31) (2018) 7884–7889, https://doi.org/10.1073/pnas.1801551115.
[23] L. Zhu, X. Chen, Delamination-Based Measurement and Prediction of the Adhesion Energy of Thin Film/Substrate Interfaces, Journal of Engineering Materials and Technology 139 (2) (2017) 021021, https://doi.org/10.1115/1.4035497.
[24] S. Deng, E. Gao, Z. Xu, V. Berry, Adhesion energy of mos2 thin films on silicon-based substrates determined via the attributes of a single mos2 wrinkle, ACS Applied Materials & Interfaces 9 (8) (2017) 7812–7818, https://doi.org/10.1021/acsami.6b16175.PMID: 28124892
[25] M. Pandey, R. Kumar, Polymer curing assisted formation of optically visible sub-micron blisters of multilayer graphene for local strain engineering, Journal of Physics: Condensed Matter 34 (24) (2022) 245401, https://doi.org/10.1088/1361-648x/ac61b4.
[26] M. Pandey, R. Ahuja, R. Kumar, Hoop compression driven instabilities in spontaneously formed multilayer graphene blisters over a polymeric substrate, Nanotechnology 34 (17) (2023) 175301, https://doi.org/10.1088/1361-6528/acaf33.
[27] L. Meng, Y. Li, T.S. Liu, C. Zhu, Q.Y. Li, X. Chen, S. Zhang, X. Zhang, L. Bao, Y. Huang, F. Xu, R.S. Ruoff, Wrinkle networks in exfoliated multilayer graphene and other layered materials, Carbon 156 (2020) 24–30, https://doi.org/10.1016/j.carbon.2019.09.035.
[28] K. Sampathkumar, C. Androulidakis, E.N. Koukaras, J. Rahova, K. Drogowska, M. Kalbac, A. Vetushka, A. Fejfar, C. Galiotis, O. Frank, Sculpturing graphene wrinkle patterns into compliant substrates, Carbon 146 (2019) 772–778, https://doi.org/10.1016/j.carbon.2019.02.041.https://www.sciencedirect.com/science/article/pii/S0008622319301654
[29] S. Luo, G. Hao, Y. Fan, L. Kou, C. He, X. Qi, C. Tang, J. Li, K. Huang, J. Zhong, Formation of ripples in atomically thin mos2 and local strain engineering of electrostatic properties, Nanotechnology 26 (10) (2015) 105705, https://doi.org/10.1088/0957-4484/26/10/105705.
[30] Z. Li, R.J. Young, D.G. Papageorgiou, I.A. Kinloch, X. Zhao, C. Yang, S. Hao, Interfacial stress transfer in strain engineered wrinkled and folded graphene, 2D Materials 6 (4) (2019) 045026, https://doi.org/10.1088/2053-1583/ab3167.
[31] F. Pizzocchero, L. Gammelgaard, B.S. Jessen, J.M. Caridad, L. Wang, J. Hone, P. Bøggild, T.J. Booth, The hot pick-up technique for batch assembly of van der waals heterostructures, Nature Communications 7 (1) (2016) 11894, https://doi.org/10.1038/ncomms11894.
[32] R. Frisenda, E. Navarro-Moratalla, P. Gant, D. Pérez De Lara, P. Jarillo-Herrero, R. V. Gorbachev, A. Castellanos-Gomez, Recent progress in the assembly of nanodevices and van der waals heterostructures by deterministic placement of 2d materials, Chem. Soc. Rev. 47 (2018) 53–68, https://doi.org/10.1039/C7CS00556C.
[33] A. Castellanos-Gomez, M. Buscema, R. Molenaar, V. Singh, L. Janssen, H.S.J. van der Zant, G.A. Steele, Deterministic transfer of two-dimensional materials by all-dry viscoelastic stamping, 2D Materials 1 (1) (2014) 011002, https://doi.org/10.1088/2053-1583/1/1/011002.
[34] V.E. Calado, G.F. Schneider, A.M.M.G. Theulings, C. Dekker, L.M.K. Vandersypen, Formation and control of wrinkles in graphene by the wedging transfer method, Applied Physics Letters 101 (10) (2012) 103116, https://doi.org/10.1063/1.4751982.
[35] A. Castellanos-Gomez, R. Roldán, E. Cappelluti, M. Buscema, F. Guinea, H.S.J. van der Zant, G.A. Steele, Local strain engineering in atomically thin mos2, Nano Letters 13 (11) (2013) 5361–5366, https://doi.org/10.1021/nl402875m.PMID: 24083520
[36] P. Xu, J. Kang, J. Suhr, J.P. Smith, K.S. Booksh, B. Wei, J. Yu, F. Li, J.-H. Byun, Y. Oh, T.-W. Chou, Spatial strain variation of graphene films for stretchable electrodes, Carbon 93 (2015) 620–624, https://doi.org/10.1016/j.carbon.2015.05.096.https://www.sciencedirect.com/science/article/pii/S0008622315005035
[37] D. Maeso, S. Pakdel, H. Santos, N. Agraït, J.J. Palacios, E. Prada, G. Rubio-Bollinger, Strong modulation of optical properties in rippled 2d gase via strain engineering, Nanotechnology 30 (24) (2019) 24LT01, https://doi.org/10.1088/1361-6528/ab0bc1.
[38] S. Deng, D. Rhee, W.-K. Lee, S. Che, B. Keisham, V. Berry, T.W. Odom, Graphene wrinkles enable spatially defined chemistry, Nano Letters 19 (8) (2019) 5640–5646, https://doi.org/10.1021/acs.nanolett.9b02178.PMID: 31268720
[39] W.-K. Lee, J. Kang, K.-S. Chen, C.J. Engel, W.-B. Jung, D. Rhee, M.C. Hersam, T. W. Odom, Multiscale, hierarchical patterning of graphene by conformal wrinkling, Nano Letters 16 (11) (2016) 7121–7127, https://doi.org/10.1021/acs.nanolett.6b03415.PMID: 27726404
[40] E. Cerda, L. Mahadevan, Geometry and physics of wrinkling, Phys. Rev. Lett. 90 (2003) 074302, https://doi.org/10.1103/PhysRevLett.90.074302.
[41] R. Yang, H. Song, Z. Zhou, S. Yang, X. Tang, J. He, S. Liu, Z. Zeng, B.-R. Yang, X. Gui, Ultra-sensitive, multi-directional flexible strain sensors based on an mxene film with periodic wrinkles, ACS Applied Materials & Interfaces 15 (6) (2023) 8345–8354, https://doi.org/10.1021/acsami.2c22158.PMID: 36725839
[42] S. Deng, E. Gao, Y. Wang, S. Sen, S.T. Sreenivasan, S. Behura, P. Král, Z. Xu, V. Berry, Confined, oriented, and electrically anisotropic graphene wrinkles on bacteria, ACS Nano 10 (9) (2016) 8403–8412, https://doi.org/10.1021/acsnano.6b03214.PMID: 27391776
[43] J. Yu, S. Kim, E. Ertekin, A.M. van der Zande, Material-dependent evolution of mechanical folding instabilities in two-dimensional atomic membranes, ACS Applied Materials & Interfaces 12 (9) (2020) 10801–10808, https://doi.org/10.1021/acsami.9b20909.PMID: 32036649
[44] S. Yang, C. Wang, H. Sahin, H. Chen, Y. Li, S.-S. Li, A. Suslu, F.M. Peeters, Q. Liu, J. Li, S. Tongay, Tuning the optical, magnetic, and electrical properties of rese2 by nanoscale strain engineering, Nano Letters 15 (3) (2015) 1660–1666, https://doi.org/10.1021/nl504276u.PMID: 25642738
[45] C. Cho, J. Wong, A. Taqieddin, S. Biswas, N.R. Aluru, S. Nam, H.A. Atwater, Highly strain-tunable interlayer excitons in mos2/wse2 heterobilayers, Nano Letters 21 (9) (2021) 3956–3964, https://doi.org/10.1021/acs.nanolett.1c00724.PMID: 33914542
[46] M. Amerian, M. Amerian, M. Sameti, E. Seyedjafari, Improvement of pdms surface biocompatibility is limited by the duration of oxygen plasma treatment, Journal of Biomedical Materials Research Part A 107 (12) (2019) 2806–2813, https://doi.org/10.1002/jbm.a.36783.
[47] Y.J. Park, S.-K. Lee, M.-S. Kim, H. Kim, J.-H. Ahn, Graphene-based conformal devices, ACS Nano 8 (8) (2014) 7655–7662, https://doi.org/10.1021/nn503446f.PMID: 25073058
[48] G. Lee, M. Zarei, Q. Wei, Y. Zhu, S.G. Lee, Surface wrinkling for flexible and stretchable sensors, Small 18 (42) (2022) 2203491, https://doi.org/10.1002/smll.202203491.
[49] X. Tang, W. Yang, S. Yin, G. Tai, M. Su, J. Yang, H. Shi, D. Wei, J. Yang, Controllable graphene wrinkle for a high-performance flexible pressure sensor, ACS Applied Materials & Interfaces 13 (17) (2021) 20448–20458, https://doi.org/10.1021/acsami.0c22784.PMID: 33899475
[50] J. Yang, Q. Ran, D. Wei, T. Sun, L. Yu, X. Song, L. Pu, H. Shi, C. Du, Three-dimensional conformal graphene microstructure for flexible and highly sensitive electronic skin, Nanotechnology 28 (11) (2017) 115501, https://doi.org/10.1088/1361-6528/aa5b56.
[51] B. Zhu, Z. Niu, H. Wang, W.R. Leow, H. Wang, Y. Li, L. Zheng, J. Wei, F. Huo, X. Chen, Microstructured graphene arrays for highly sensitive flexible tactile sensors, Small 10 (18) (2014) 3625–3631, https://doi.org/10.1002/smll.201401207.
[52] S. Zhang, C. Ge, R. Liu, Mechanical characterization of the stress-strain behavior of the polydimethylsiloxane (pdms) substate of wearable strain sensors under uniaxial loading conditions, Sensors and Actuators A: Physical 341 (2022) 113580, https://doi.org/10.1016/j.sna.2022.113580.https://www.sciencedirect.com/science/article/pii/S0924424722002187
[53] C. Androulidakis, E.N. Koukaras, J. Rahova, K. Sampathkumar, J. Parthenios, K. Papagelis, O. Frank, C. Galiotis, Wrinkled few-layer graphene as highly efficient load bearer, ACS Applied Materials & Interfaces 9 (31) (2017) 26593–26601, https://doi.org/10.1021/acsami.7b07547.PMID: 28722403
[54] S. Deng, V. Berry, Wrinkled, rippled and crumpled graphene: an overview of formation mechanism, electronic properties, and applications, Materials Today 19 (4) (2016) 197–212, https://doi.org/10.1016/j.mattod.2015.10.002.https://www.sciencedirect.com/science/article/pii/S1369702115003119
[55] M. Moun, A. Vasdev, R. Pujar, K. Priya Madhuri, U. Mogera, N.S. John, G. U. Kulkarni, G. Sheet, Enhanced electrical transport through wrinkles in turbostratic graphene films, Applied Physics Letters 119 (3) (2021) 033102, https://doi.org/10.1063/5.0056212.
[56] S. Chun, Y. Choi, W. Park, All-graphene strain sensor on soft substrate, Carbon 116 (2017) 753–759, https://doi.org/10.1016/j.carbon.2017.02.058.https://www.sciencedirect.com/science/article/pii/S0008622317301872

[57] T. Liang, W. Hou, J. Ji, Y. Huang, Wrinkled reduced graphene oxide humidity sensor with fast response/recovery and flexibility for respiratory monitoring, Sensors and Actuators A: Physical 350 (2023) 114104, https://doi.org/10.1016/j.sna.2022.114104.https://www.sciencedirect.com/science/article/pii/S0924424722007397
[58] L. Wang, S. Qiao, S. Kabiri Ameri, H. Jeong, N. Lu, A Thin Elastic Membrane Conformed to a Soft and Rough Substrate Subjected to Stretching/Compression, Journal of Applied Mechanics 84 (11) (2017) 111003, https://doi.org/10.1115/1.4037740.
[59] L. Wang, N. Lu, Conformability of a Thin Elastic Membrane Laminated on a Soft Substrate With Slightly Wavy Surface, Journal of Applied Mechanics 83 (4) (2016) 041007, https://doi.org/10.1115/1.4032466.
[60] W. Gao, R. Huang, Effect of surface roughness on adhesion of graphene membranes, Journal of Physics D: Applied Physics 44 (45) (2011) 452001, https://doi.org/10.1088/0022-3727/44/45/452001.
[61] W. Zhu, T. Low, V. Perebeinos, A.A. Bol, Y. Zhu, H. Yan, J. Tersoff, P. Avouris, Structure and electronic transport in graphene wrinkles, Nano Letters 12 (7) (2012) 3431–3436, https://doi.org/10.1021/nl300563h.PMID: 22646513
[62] Z. Zhang, T. Li, Determining graphene adhesion via substrate-regulated morphology of graphene, Journal of Applied Physics 110 (8) (2011) 083526, https://doi.org/10.1063/1.3656720.
[63] S. Scharfenberg, D.Z. Rocklin, C. Chialvo, R.L. Weaver, P.M. Goldbart, N. Mason, Probing the mechanical properties of graphene using a corrugated elastic substrate, Applied Physics Letters 98 (9) (2011) 091908, https://doi.org/10.1063/1.3553228.
[64] S. Scharfenberg, N. Mansukhani, C. Chialvo, R.L. Weaver, N. Mason, Observation of a snap-through instability in graphene, Applied Physics Letters 100 (2) (2012) 021910, https://doi.org/10.1063/1.3676059.
[65] T.J.W. Wagner, D. Vella, The sensitivity of graphene snap-through to substrate geometry, Applied Physics Letters 100 (23) (2012) 233111, https://doi.org/10.1063/1.4724329.
[66] T. Li, Z. Zhang, Substrate-regulated morphology of graphene, Journal of Physics D: Applied Physics 43 (7) (2010) 075303, https://doi.org/10.1088/0022-3727/43/7/075303.
[67] C. Ma, Y. Zhang, S. Jiao, M. Liu, Snap-through of graphene nanowrinkles under out-of-plane compression, Nanotechnology 34 (1) (2022) 015705, https://doi.org/10.1088/1361-6528/ac9418.
[68] T. Li, Z. Zhang, Snap-through instability of graphene on substrates, Nanoscale Research Letters 5 (1) (2009) 169, https://doi.org/10.1007/s11671-009-9460-1.
[69] M. Gomez, D. Moulton, D. Vella, Critical slowing down in purely elastic 'snap-through' instabilities, Nature Physics 13 (2) (2017) 142–145, https://doi.org/10.1038/nphys3915.
[70] C. Androulidakis, E.N. Koukaras, M.G. Pastore Carbone, M. Hadjinicolaou, C. Galiotis, Wrinkling formation in simply-supported graphenes under tension and compression loadings, Nanoscale 9 (2017) 18180–18188, https://doi.org/10.1039/C7NR06463B.
[71] M. Neek-Amal, F.M. Peeters, Strain-engineered graphene through a nanostructured substrate. i. deformations, Phys. Rev. B 85 (2012) 195445, https://doi.org/10.1103/PhysRevB.85.195445.
[72] X. He, Q. Bai, R. Shen, F. Zhang, Y. Guo, The evolution of configuration and final state of graphene on rough iron surface, Applied Surface Science 530 (2020) 147084, https://doi.org/10.1016/j.apsusc.2020.147084.https://www.sciencedirect.com/science/article/pii/S0169433220318419
[73] E. Okogbue, J.H. Kim, T.-J. Ko, H.-S. Chung, A. Krishnaprasad, J.C. Flores, S. Nehate, M.G. Kaium, J.B. Park, S.-J. Lee, K.B. Sundaram, L. Zhai, T. Roy, Y. Jung, Centimeter-scale periodically corrugated few-layer 2d mos2 with tensile stretch-driven tunable multifunctionalities, ACS Applied Materials & Interfaces 10 (36) (2018) 30623–30630, https://doi.org/10.1021/acsami.8b08178.PMID: 30059199
[74] Y. Jin, Q. Ren, J. Liu, Y. Zhang, H. Zheng, P. Zhao, Stretching graphene to 3.3% strain using formvar-reinforced flexible substrate, Experimental Mechanics 62 (5) (2022) 761–767, https://doi.org/10.1007/s11340-021-00817-3.
[75] C. Xu, T. Xue, J. Guo, Q. Qin, S. Wu, H. Song, H. Xie, An experimental investigation on the mechanical properties of the interface between large-sized graphene and a flexible substrate, Journal of Applied Physics 117 (16) (2015) 164301, https://doi.org/10.1063/1.4918899.
[76] S. Lee, E. Byeon, S. Jung, D.-G. Kim, Heterogeneity of hard skin layer in wrinkled pdms surface fabricated by ar ion-beam irradiation, Scientific Reports 8 (1) (2018) 14063, https://doi.org/10.1038/s41598-018-32378-2.
[77] H.-C. Jeong, H.-G. Park, Y.H. Jung, J.H. Lee, B.-Y. Oh, D.-S. Seo, Tailoring the orientation and periodicity of wrinkles using ion-beam bombardment, Langmuir 32 (28) (2016) 7138–7143, https://doi.org/10.1021/acs.langmuir.6b01473.PMID: 27322365
[78] H.-C. Jeong, H.-G. Park, J.H. Lee, D.-S. Seo, Localized ion-beam irradiation-induced wrinkle patterns, ACS Applied Materials & Interfaces 7 (41) (2015) 23216–23222, https://doi.org/10.1021/acsami.5b07147.PMID: 26430969
[79] S.F. Ahmed, G.-H. Rho, K.-R. Lee, A. Vaziri, M.-W. Moon, High aspect ratio wrinkles on a soft polymer, Soft Matter 6 (2010) 5709–5714, https://doi.org/10.1039/C0SM00386G.
[80] V. Pachchigar, M. Ranjan, S. Mukherjee, Role of hierarchical protrusions in water repellent superhydrophobic ptfe surface produced by low energy ion beam irradiation, Scientific Reports 9 (1) (2019) 8675, https://doi.org/10.1038/s41598-019-45132-z.
[81] Y.H.J..D.-S.S. Hong-Gyu Park Hae-Chang Jeong, Control of the wrinkle structure on surface-reformed poly(dimethylsiloxane) via ion-beam bombardment, Sci Rep 5 (5) (2015) 12356, https://doi.org/10.1038/srep12356.PMID: 33914542
[82] J.-K. Lee, S. Yamazaki, H. Yun, J. Park, G.P. Kennedy, G.-T. Kim, O. Pietzsch, R. Wiesendanger, S. Lee, S. Hong, U. Dettlaff-Weglikowska, S. Roth, Modification of electrical properties of graphene by substrate-induced nanomodulation, Nano Letters 13 (8) (2013) 3494–3500, https://doi.org/10.1021/nl400827p.PMID: 23848516
[83] H. Mei, R. Huang, J.Y. Chung, C.M. Stafford, H.-H. Yu, Buckling modes of elastic thin films on elastic substrates, Applied Physics Letters 90 (15) (2007) 151902, https://doi.org/10.1063/1.2720759.
[84] R.M. Bradley, J.M.E. Harper, Theory of ripple topography induced by ion bombardment, Journal of Vacuum Science & Technology A 6 (4) (1988) 2390–2395, https://doi.org/10.1116/1.575561.
[85] N.G. Boddeti, R. Long, M.L. Dunn, Adhesion mechanics of graphene on textured substrates, International Journal of Solids and Structures 97-98 (2016) 56–74, https://doi.org/10.1016/j.ijsolstr.2016.07.043.https://www.sciencedirect.com/science/article/pii/S0020768316302049
[86] D. Ru, C. Zhu, S. Dong, J. Zhao, Wrinkling behavior of graphene on substrates with different surface morphologies, Mechanics of Materials 137 (2019) 103144, https://doi.org/10.1016/j.mechmat.2019.103144.https://www.sciencedirect.com/science/article/pii/S0167663619305551
[87] Z. Wang, D. Tonderys, S.E. Leggett, E.K. Williams, M.T. Kiani, R. Spitz Steinberg, Y. Qiu, I.Y. Wong, R.H. Hurt, Wrinkled, wavelength-tunable graphene-based surface topographies for directing cell alignment and morphology, Carbon 97 (2016) 14–24, https://doi.org/10.1016/j.carbon.2015.03.040.BIOMEDICAL APPLICATIONS OF CARBON NANOMATERIALS
[88] G. Wang, Z. Dai, J. Xiao, S. Feng, C. Weng, L. Liu, Z. Xu, R. Huang, Z. Zhang, Bending of multilayer van der waals materials, Phys. Rev. Lett. 123 (2019) 116101, https://doi.org/10.1103/PhysRevLett.123.116101.
[89] E. Han, J. Yu, E. Annevelink, J. Son, D.A. Kang, K. Watanabe, T. Taniguchi, E. Ertekin, P.Y. Huang, A.M. van der Zande, Ultrasoft slip-mediated bending in few-layer graphene, Nature Materials 19 (3) (2020) 305–309, https://doi.org/10.1038/s41563-019-0529-7.
[90] S. Viola Kusminskiy, D.K. Campbell, A.H. Castro Neto, F. Guinea, Pinning of a two-dimensional membrane on top of a patterned substrate: The case of graphene, Phys. Rev. B 83 (2011) 165405, https://doi.org/10.1103/PhysRevB.83.165405.
[91] S.P. Koenig, N.G. Boddeti, M.L. Dunn, J.S. Bunch, Ultrastrong adhesion of graphene membranes, Nature Nanotechnology 6 (9) (2011) 543–546, https://doi.org/10.1038/nnano.2011.123.
[92] H. Du, T. Xue, C. Xu, Y. Kang, W. Dou, Improvement of mechanical properties of graphene/substrate interface via regulation of initial strain through cyclic loading, Optics and Lasers in Engineering 110 (2018) 356–363, https://doi.org/10.1016/j.optlaseng.2018.04.026.https://www.sciencedirect.com/science/article/pii/S0143816618300836
[93] T.M.G. Mohiuddin, A. Lombardo, R.R. Nair, A. Bonetti, G. Savini, R. Jalil, N. Bonini, D.M. Basko, C. Galiotis, N. Marzari, K.S. Novoselov, A.K. Geim, A. C. Ferrari, Uniaxial strain in graphene by raman spectroscopy:g peak splitting, grüneisen parameters, and sample orientation, Phys. Rev. B 79 (2009) 205433, https://doi.org/10.1103/PhysRevB.79.205433.
[94] D. Rhee, J.T. Paci, S. Deng, W.-K. Lee, G.C. Schatz, T.W. Odom, Soft skin layers enable area-specific, multiscale graphene wrinkles with switchable orientations, ACS Nano 14 (1) (2020) 166–174, https://doi.org/10.1021/acsnano.9b06325.PMID: 31675210
[95] Z. Huang, A. Alharbi, W. Mayer, E. Cuniberto, T. Taniguchi, K. Watanabe, J. Shabani, D. Shahrjerdi, Versatile construction of van der waals heterostructures using a dual-function polymeric film, Nature Communications 11 (1) (2020) 3029, https://doi.org/10.1038/s41467-020-16817-1.